Electronic Supplementary Material (ESI) for Catalysis Science & Technology.
This journal is © The Royal Society of Chemistry 2020

D-Phenylglycine aminotransferase (D-PhgAT) – substrate scope and structural insights of a stereo-inverting biocatalyst used in the preparation of aromatic amino acid

Supplementary Information

Annabel Serpico, Silvia De Cesare, Jon Marles-Wright, M. Kalim Akhtar, Gary J. Loake, Dominic J. Campopiano*

Supplementary Method

Site directed mutagenesis

The D-PhgAT R34A, H66A, H213A, Q301A and R407A mutants were constructed according to the overlapping primer site-directed mutagenesis (SDM) method with the primer pairs outlined below.

R34A:
R34A forward (5'- ATGGCGTGACCGCGGACACCGCTGTGTTCGAT-3')
R34A reverse (5'- ACAGACCGTGCGGATCGAACAC**AGC**GGTGTCCG C-3')
H66A:
H66A forward (5'-CTTTGGTGGCGCTGGTGCGCTGGTGCTG-3')
H66A reverse (5'-GCGCACCAGCGCCACCAAAGAA ATCCAG-3')
H213A:
H213A forward (5'-CGGTTGGTAGCGCCTTTGGCTGACCCCGG-3')
H213A reverse (5'-CACGCCAAAGGCGCTACCAACCGGTTCC -3')
Q300A:
Q300A forward (5'-TGCTGCACGCGGGTACCTTCACCGG-3')
Q300A reverse (5'-AAGGTACCCTCCGCGTGCAGCACTTTACGAT-3')
R407A:
R407A forward (5'-CATCGGTGGCGCTGGCAGCGTTTTTCTGAGCGCG-3')
R407A reverse (5'-AAAACGCTGCCAGCGCCACCGATGTCCACACCTT-3')

Colonies were picked and sequenced, and based on the results, mutants were taken forward for analysis. The mass of each D-PhgAT mutant was confirmed by LC electrospray ionization mass spectrometry (ESI–MS).

Supplementary Figures

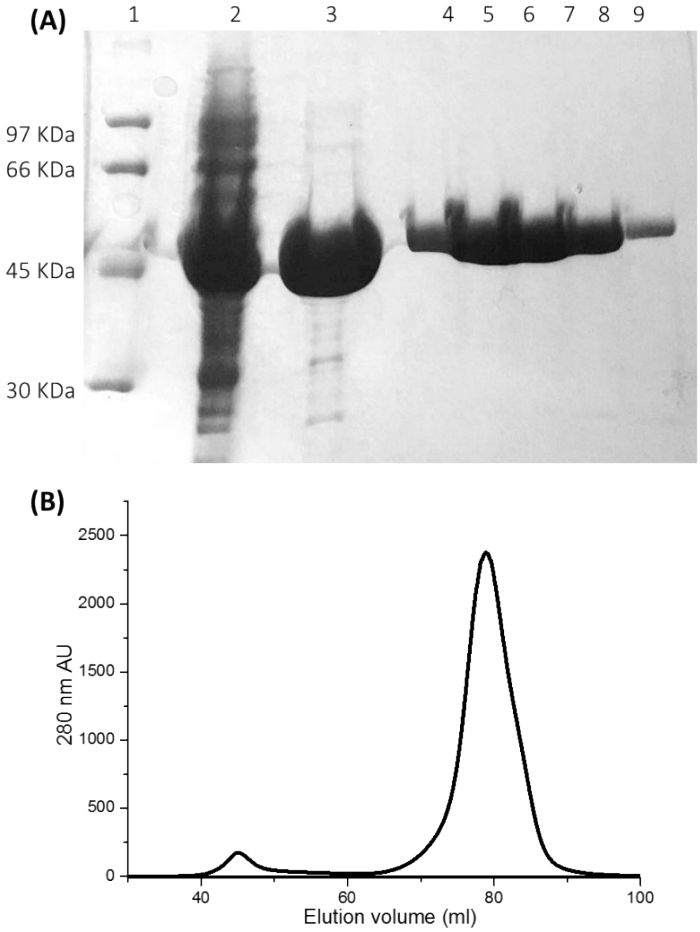

Figure S1. (a) 10% SDS-PAGE analysis of D-PhgAT purification steps. Lane1: low molecular weight marker (GE Healthcare LMWM); Lane 2: Soluble fraction of cell lysate; Lane 3: D-PhgAT elution fraction after nickel affinity purification; Lanes 4-9: fractions from Superdex S200 HR gel filtration chromatography (3 mL fractions from 69-87 mL), (**b**) chromatogram of fractions from the Superdex S200 HR column of D-PhgAT (1 mL/min using 0.1 M CAPS, 150 mM NaCl pH 9.5).

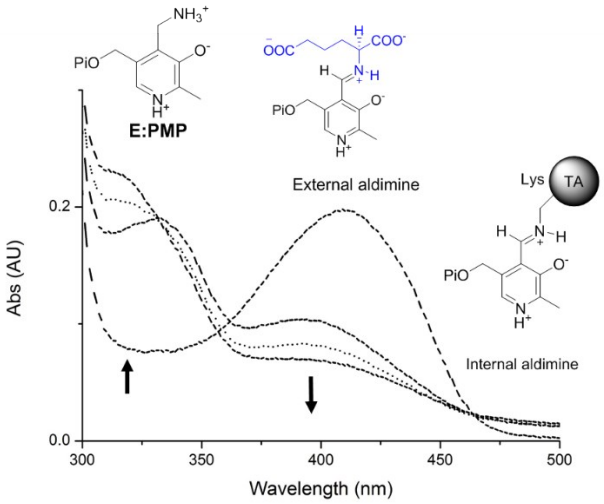

Figure S2. UV-Visible spectroscopy analysis of pure, PLP-bound D-PhgAT and after the addition of L-Glu (1 mM). The 411 nm peak, corresponding to the PLP-bound, internal aldimine, disappears and a peak at 330 nm, corresponding to the PLP:L-glu external aldimine is observed. After ~30mins a further shift towards 314 nm suggests the production of the non-covalently-bound D-PhgAT:PMP complex form of the enzyme.

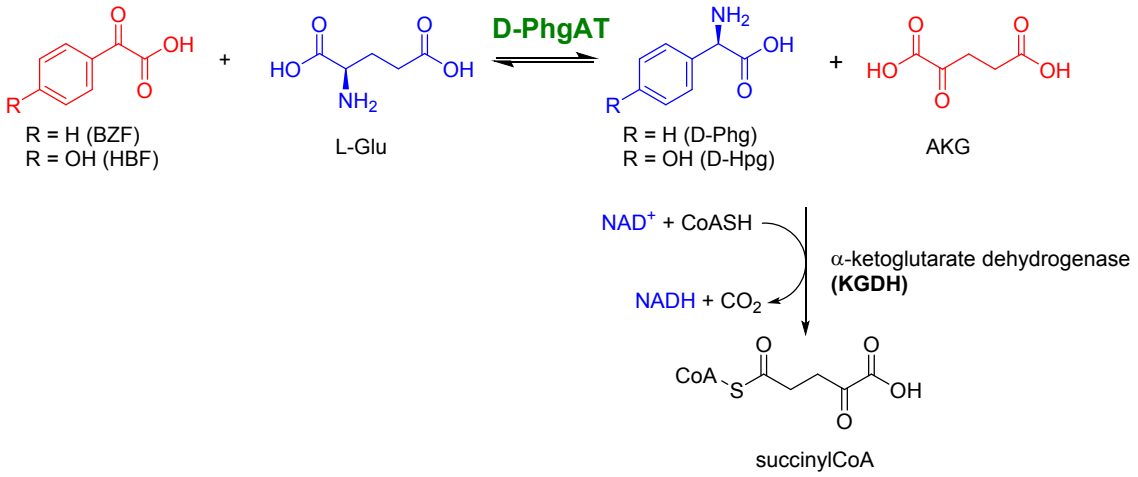

Figure S3. Reaction scheme for the D-PhgAT/α–ketoglutarate dehydrogenase (AKGDH) coupled assay. The α–ketoglutarate (AKG) product of the first half of the transamination reaction is converted by the AKGDH to produce succinyl-CoA and NADH, whose production can be monitored at 340 nm (ε_{340} = 6220 $M^{-1}cm^{-1}$).

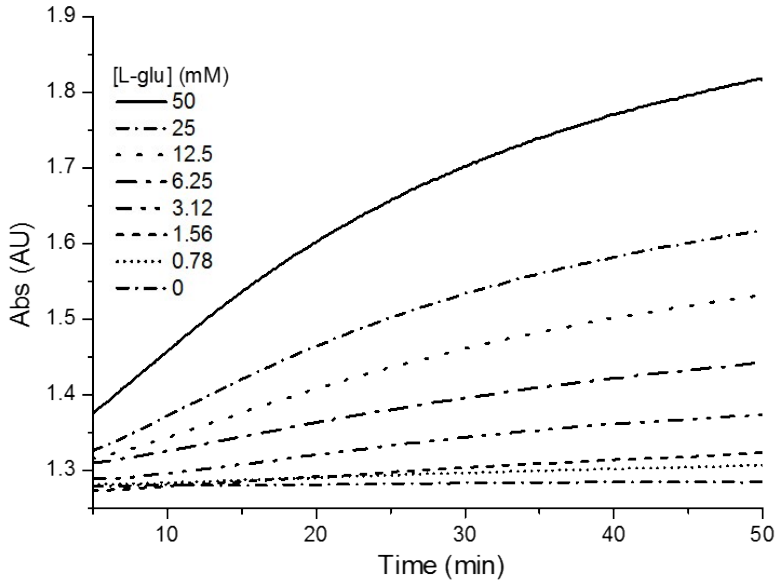

Figure S4. Typical progress curve of the AKGDH assay monitoring the NADH appearance at 340 nm. Several L-glu concentrations (0-100 mM) were tested keeping the [BZF] constant at 10 mM. The initial rate (over ~15 min) was used to calculate kinetic parameters by non-linear regression using Origin software.

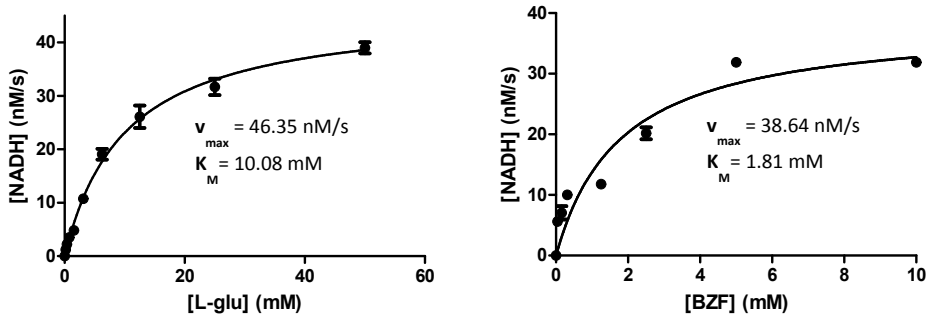

Figure S5. Michaelis Menten plots of the kinetic reactions for the two natural substrates L glu, BZF, using the AKG coupled assay. Data was analysed by non-linear regression using Origin software. NADH extinction coefficient 6220 M^{-1} cm^{-1}.

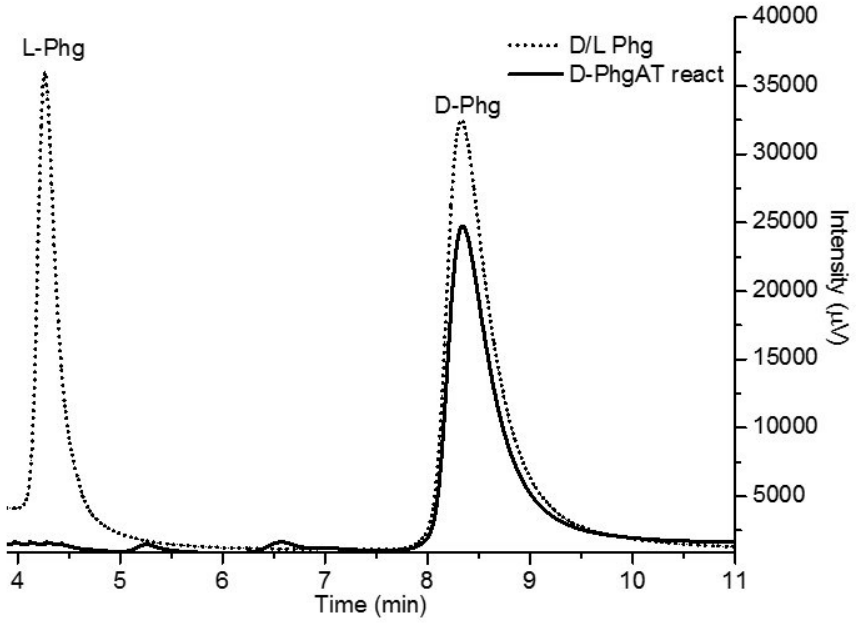

Figure S6. Enantioselectivity of the D-PhgAT reaction. Chiral HPLC analysis of the L- and D-Phg standards (5 mM, elution at 4.3 min and 8.3 min respectively, dashes). The D-PhgAT reaction carried out overnight at 37°C (100 mM L-glu, 10 mM BZF, 100 mM CAPS, pH 9.5) shows the formation of only the D-Phg enantiomer (solid line).

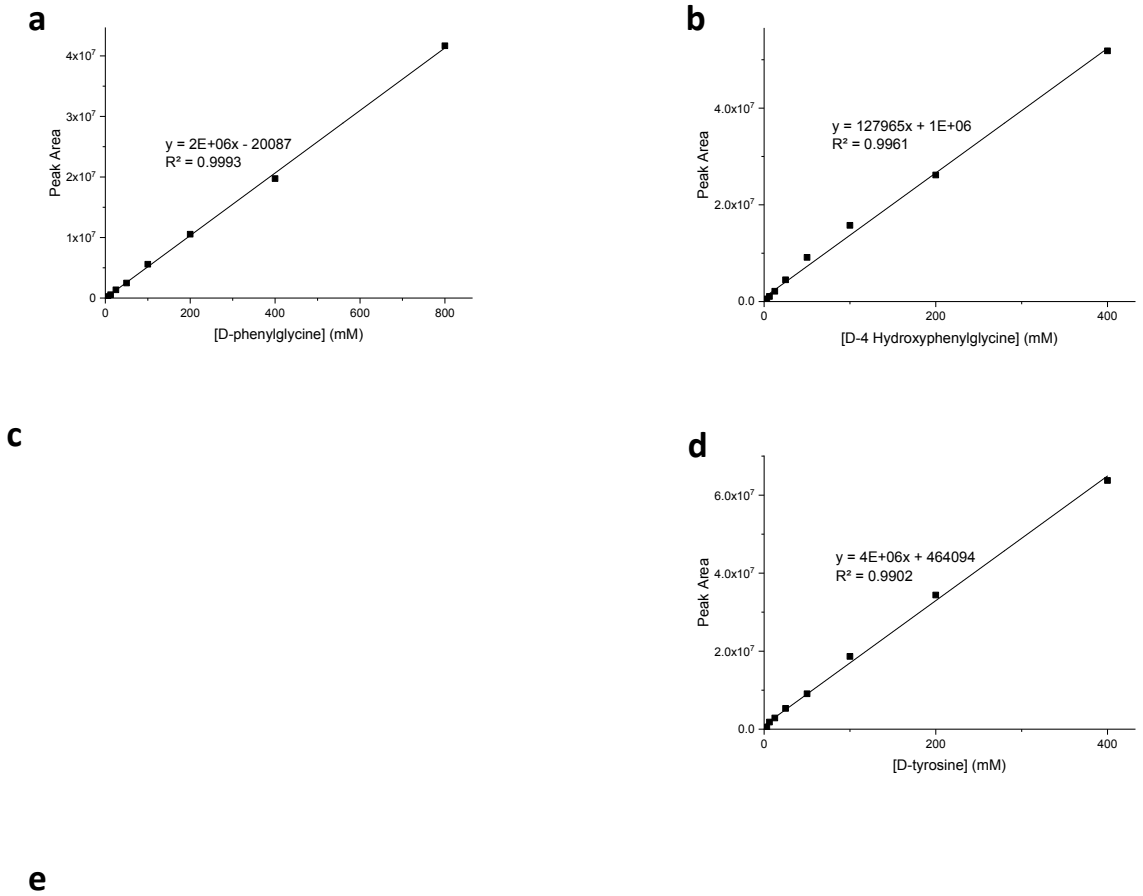

Figure S7. Calibration of chiral HPLC analysis using a Chirobiotic T column. Each amino acid concentration (0 – 400 mM) was analysed using the following solvents (0.025% triethylammonium acetate (TEAA):MeOH (50:50). The flow rate was 1 mL/min with elution monitored at λ = 205 nm. The calibration curves of: a) D-phenylgylcine b) D-4 hydroxyphenylglycine c) D- phenylalanine d) D-tyrosine e) D-tryptophan were fit with linear regression on Origin.

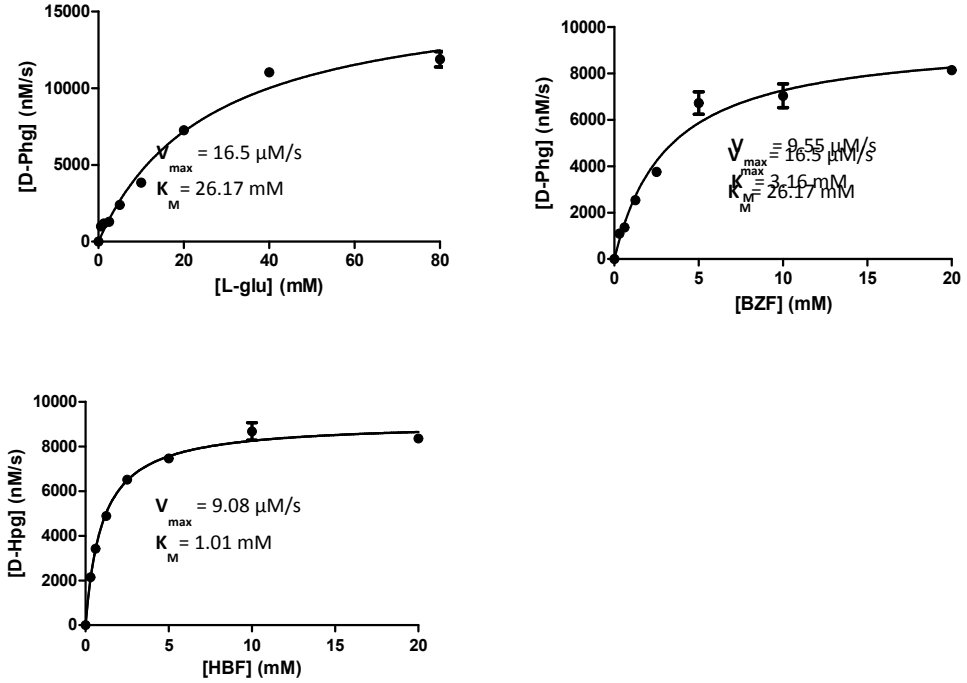

Figure S8. Michaelis Menten plots of the kinetic reactions for the three natural substrates L-Glu, BZF, HBF. Product formation was monitored using the Chiral HPLC method and data was analysed by non-linear regression using Origin software.

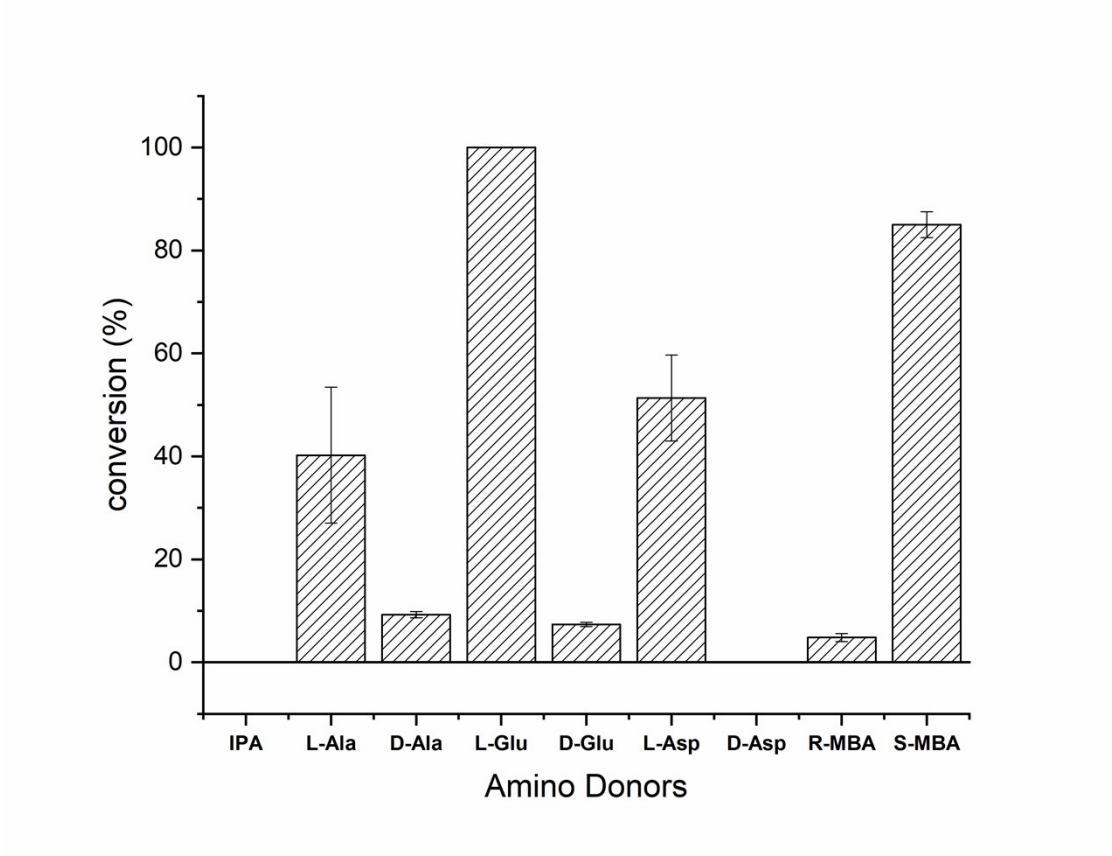

Figure S9. Comparison of D-Phg production with various L- and D- amine donors. The amino donors (IPA, L-Ala and D-Ala, L-Glu and D-Glu, L-Asp and D-Asp, *R*-MBA and *S*-MBA) and amino acceptor (BZF) were all at 10 mM. All reactions were carried out for 18 h in parallel and the results are shown as percentage conversion relative to L-Glu.

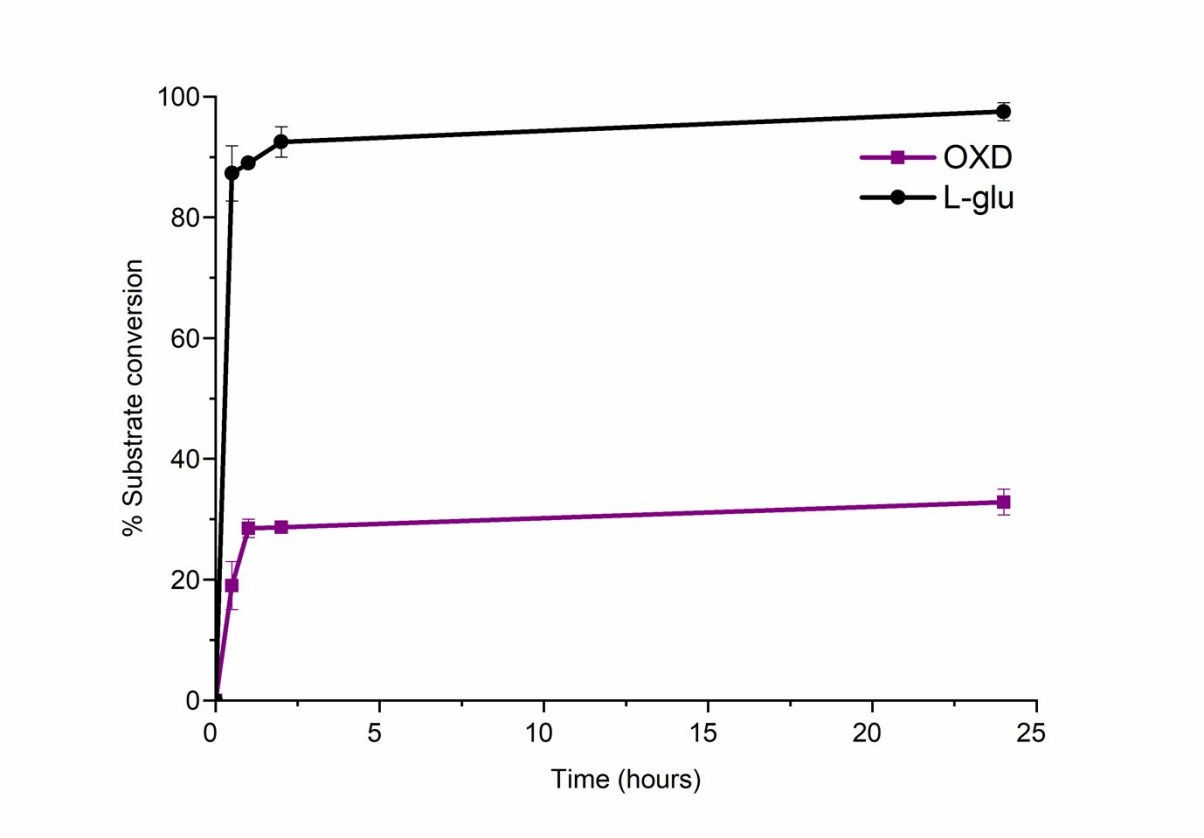

Figure S10. Comparison of D-Phg production with amine donors L-Glu and the xenobiotic *o*-xylene diamine (OXD). Reactions were carried out as described for figure S9.

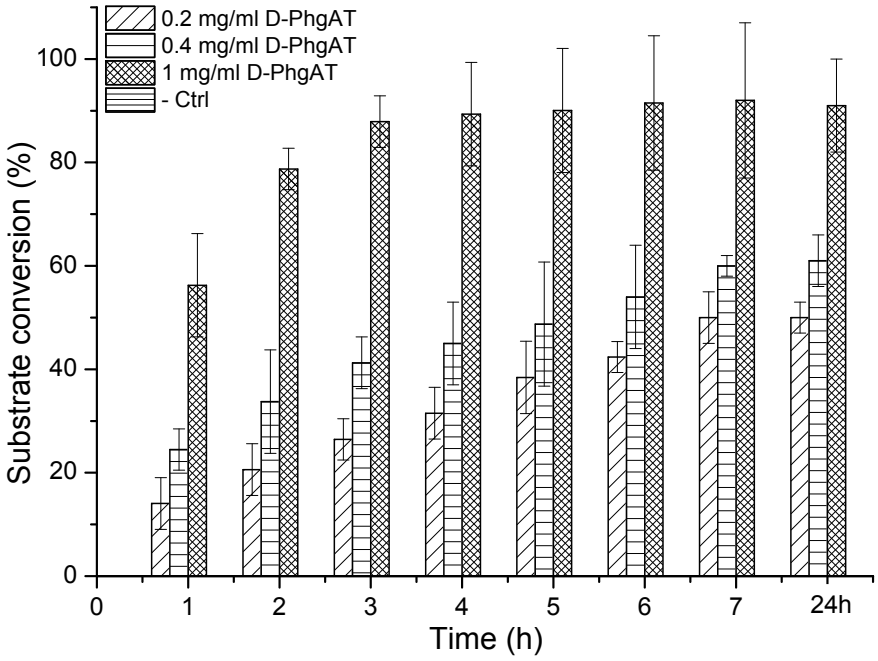

Figure S11. Biotransformation reactions using D-PhgAT and 1 g BZF. Different enzyme concentrations (0.2 -1.0 mg/mL) were compared at different time points. 1 mg/mL of D-PhgAT showed 93% conversion (> 99% ee) after reaction for 3 hours. Product formation was monitored using the Chiral HPLC method.

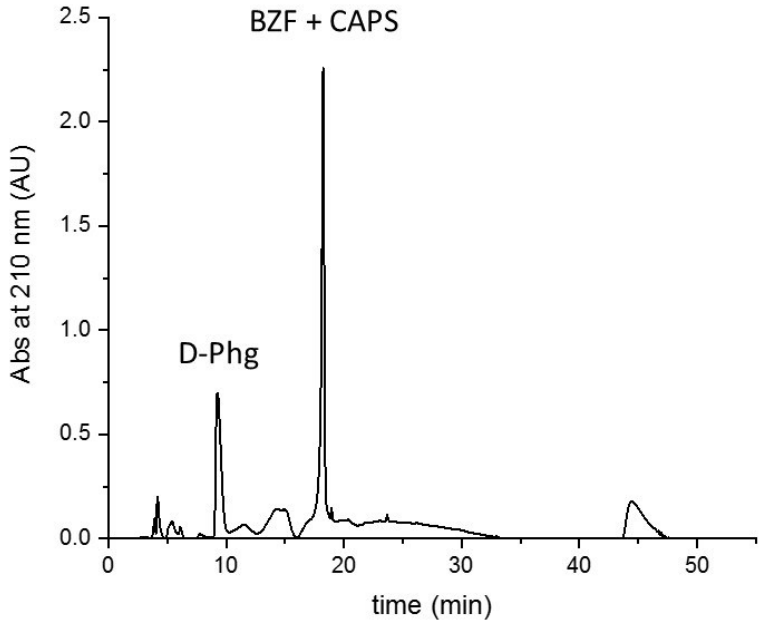

Figure S12. Isolation of D-Phg from the 1 g scale D-PhgAT catalyzed biotransformation reaction. Reaction conditions were as follows (in 50 mL, BZF (1g, 133 mM), L-Glu (500 mM), D-PhgAT (50 mg or 1 mg/mL) in CAPS buffer (100 mM, pH 9.5). The reaction was incubated for 36 hours at 37 °C with shaking (at 120 rpm). The reaction mixture was centrifuged at 10000 rpm and the supernatant collected and freeze dried. 100 mg of crude reaction mixture was dissolved in 1 mL of water and filtered using a 0.2 μM filter. Isolation of D-Phg was carried out on a preparative HPLC (Phenomenex C18 Preparative column, 250 x 21.20 mm, 5 μ), at a flow rate of 18 mL/min, isocratic run 95 % water 0.1 % TFA + 5 % AcCN 0.1 % TFA. 250 μL of sample was injected on the column and the product eluted after 9 minutes (abs at 210 nm). After four consecutive injections the fractions containing D-Phg were combined, freeze dried and characterised by NMR and MS. Product formation was monitored using the chiral HPLC method.

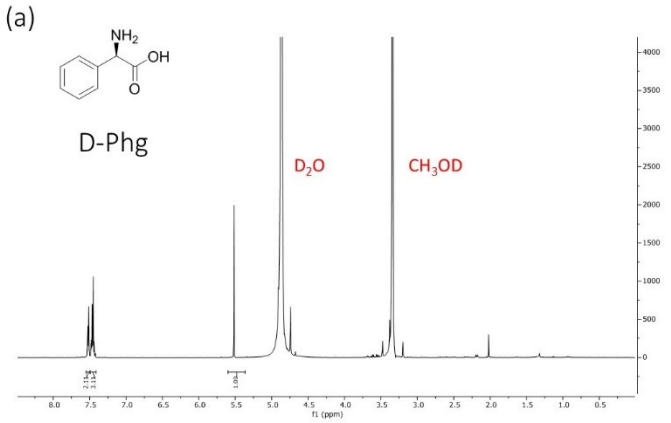

^{1}H NMR (500 MHz, D_2O/MeOD) = 7.52 (m, 2H), 7.46 (m, 3H) and 5.5 (s, 1H)

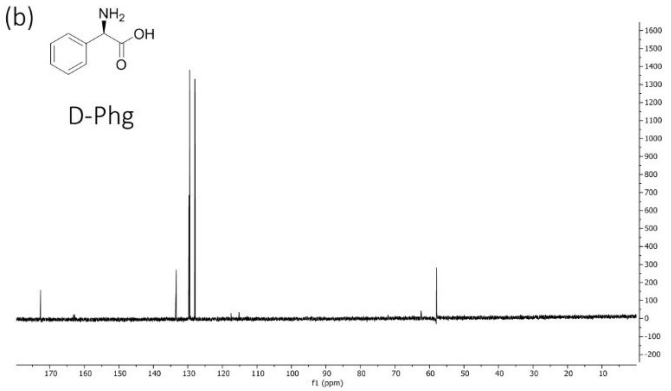

^{13}C NMR (133 MHz, D_2O) = 172.67, 133.41, 129.72, 129.45, 127.96 and 58.00

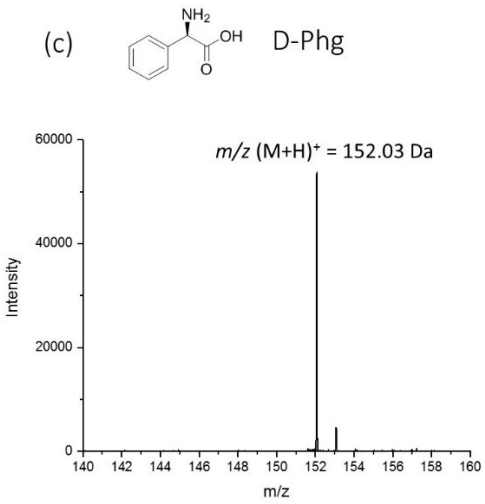

Figure S13. Characterisation of D-Phg isolated from the biotransformation. (a) ^{1}H NMR analysis, 500 MHz (b) ^{13}C NMR, Bruker Ascend 500 MHz (c) Electrospray ionisation mass spectrum (ESI-MS). Carried out on a Micro-TofII Bruker MS by direct injection. Predicted mass ($C_8H_9NO_2$) = 151.06; observed mass, $(M+H)^+$ = 152.03.

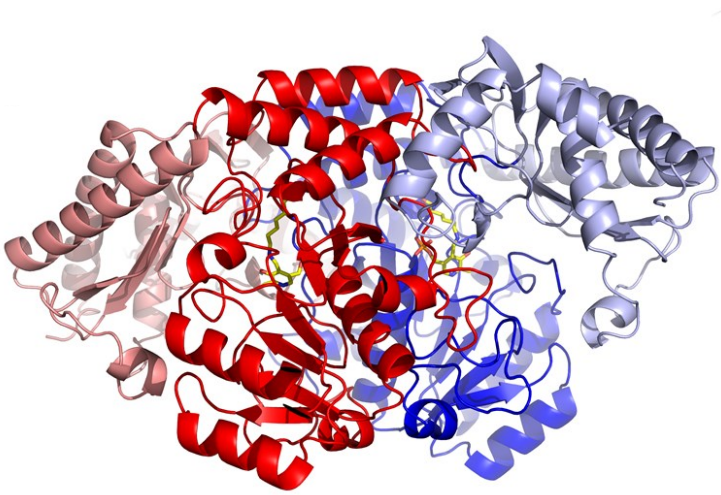

Figure S14. Overall architecture of the DphgAT dimer. The crystal structure of the D-PhgAT homo-dimer with PLP internal aldimine at 2.25 Å resolution. The small domain of monomer A is in light red while the large domain is in red. The small domain of monomer B is in light blue while the large domain is in blue. The PLP cofactor is in yellow.

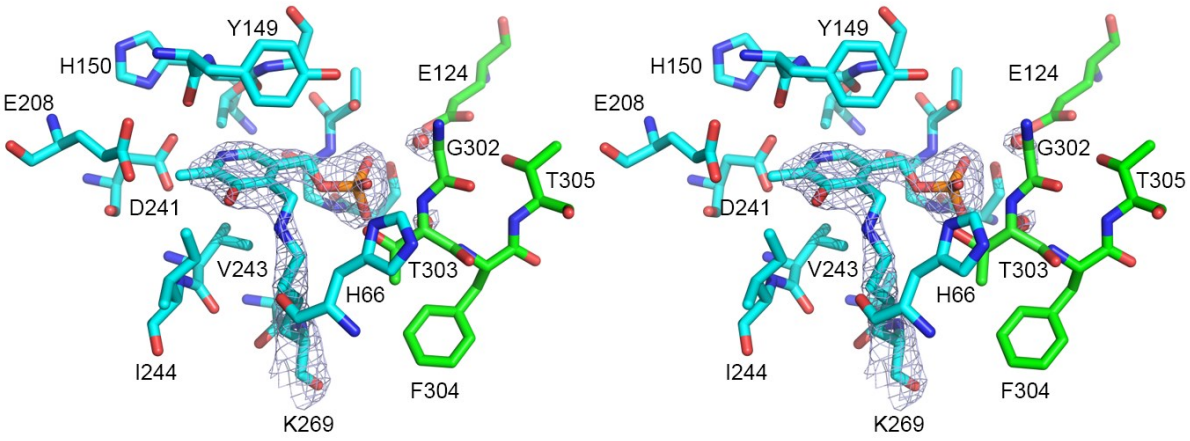

Figure S15. Wall-eyed stereo-view of the experimental electron density map of D-PhgAT PLP internal aldimine. The final 2mFo-DFc electron density map is shown at 1.5 σ. The side-chains involved in cofactor binding are shown as stick models (cyan for monomer A and green for monomer B). Residues involved in PLP ring interactions include Tyr149, Asp241 and Val243. Water molecules (red spheres) form bridges between the phosphate oxygens and the side chains of Glu124, Thr303 and the backbone of Phe304 from the opposite monomer. The phosphate is also coordinated by H-bonds to Ser121, Gly122 and Thr123 from the same monomer (omitted for clarity).

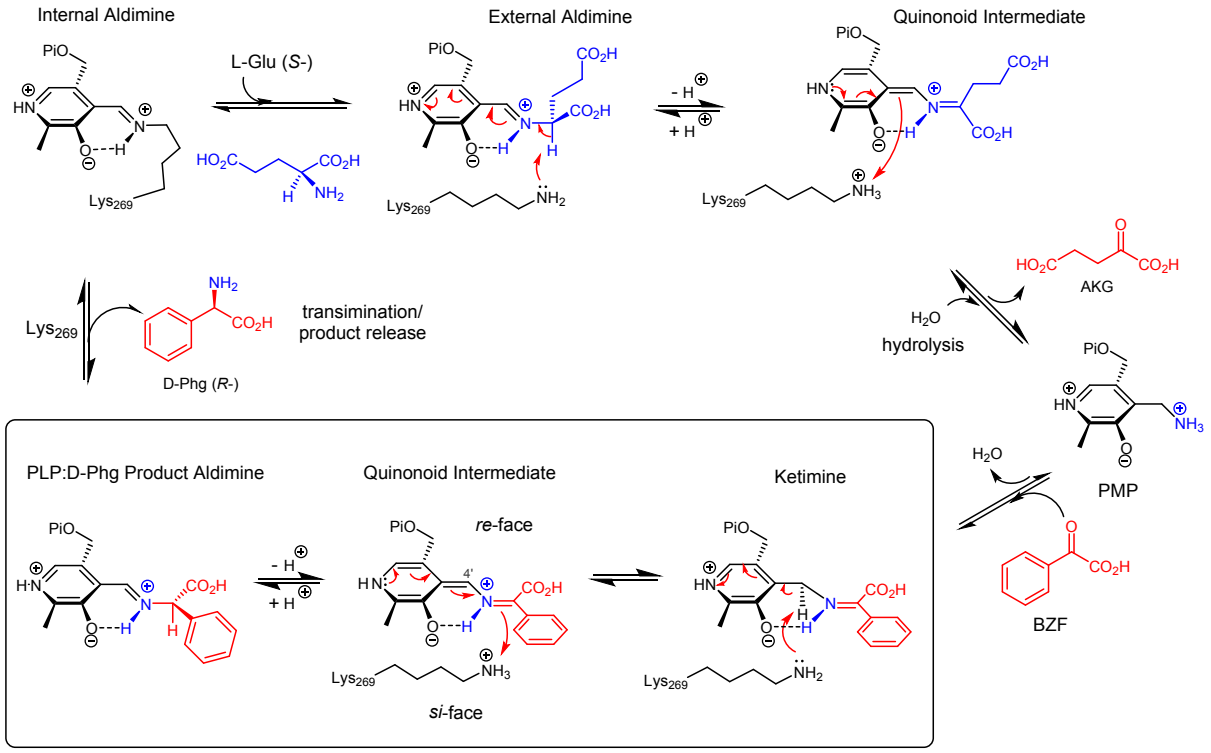

Figure S16. Stereo-inverting reaction mechanism for the D-PhgAT-catalysed D-Phg formation reaction using L-Glu as amino donor and BZF as amino acceptor. The L-Glu amino donor is shown in blue while the BZF is shown in red. The key step in determining the enzyme enantioselectivity that generates the D-Phg is the proton transfer of the planar quinonoid intermediate at C-4' by the lysine 269 which happens from only one face, the *si*-face (boxed).

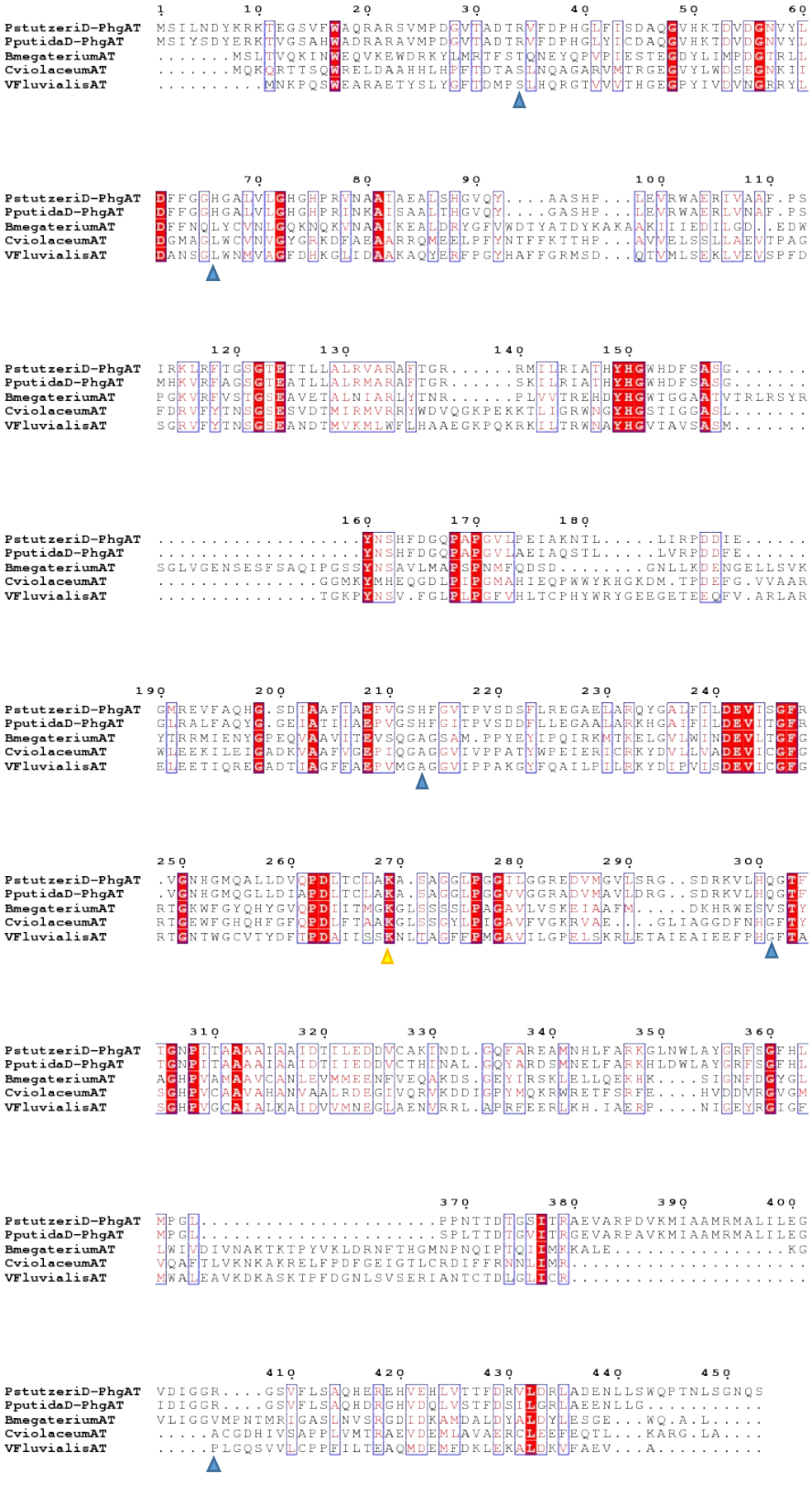

Figure S17. Multiple sequence alignment of *P. stutzeri* D-PhgAT (Uniprot code: Q6VY99) and *P. putita* D-PhgAT (extracted from Genbank: AX467211) with related S-selective Class III ATs. The sequences are *Bacillus megaterium* AT (**A0A1C7D190)**, *Vibrio fluvialis* AT (F2XBU9), *Chromobacterium violaceum* (Q7NWG4). The D-PhgAT specific residues Arg34, His66, His213, Gln301 and Arg407 proposed to be

involved in substrate orientation, dual substrate specificity and D-amino acid product formation are marked with a blue triangle. The conserved Lys269 residue is marked with a yellow triangle. Figure prepared with ESPript3.

Supplementary Tables

AKG assay				Chiral HPLC		
K_M (mM)	k_{cat} (s^{-1})	k_{cat}/K_M ($M^{-1}s^{-1}$)	Substrate	K_M (mM)	k_{cat} (s^{-1})	k_{cat}/K_M (M^{-1} s^{-1})
1.81 ± 0.57	0.39± 0.072	213.72± 0.49	**BZF**	3.16 ± 0.46	0.95 ± 0.056	302.80 ± 0.10
NA	NA	NA	**HBF**	1.01 ± 0.07	0.91 ± 0.022	899.15 ± 0.27
9.85 ± 0.62	0.46 ±0.011	46.65 ±0.32	**L-Glu**	26.17 ± 3.63	1.65 ± 0.12	63.21 0.78

Table S1. Summary of D-PhgAT kinetic parameters towards natural substrate calculated with both spectrophotometric and HPLC approaches.

	D-PhgAT
Data collection	
Wavelength (Å)	0.9795
Resolution range (Å)	49.47 - 2.248 (2.329 - 2.248)
Space group	C 1 2 1
Unit cell (Å)	*a* = 329.28, *b* = 83.90, *c* = 133.42
Unit cell (°)	β = 111.56
Total reflections	60,0728 (56,842)
Unique reflections	160,521 (15,800)
Multiplicity	3.7 (3.6)
Completeness (%)	99.76 (98.19)
Mean I/sigma(I)	12.70 (1.39)
Wilson B-factor (Å^2)	48.16
R_{merge}	0.062 (0.869)
R_{meas}	0.072 (1.018)
R_{pim}	0.037 (0.522)
$CC_{1/2}$	0.998 (0.609)
CC*	1 (0.87)
Diffraction images (DOI)	10.5281/zenodo.1059413
Refinement	
Reflections used in refinement	160,770 (15,797)
Reflections used for R_{free}	8,144 (782)
R_{work}	0.1828 (0.2874)
R_{free}	0.2106 (0.3125)
CC(work)	0.963 (0.794)
CC(free)	0.952 (0.763)
Number of non-hydrogen atoms	20,642
macromolecules	20,233
solvent	409
Protein residues	2641
RMS (bonds) (Å)	0.004
RMS (angles) (°)	0.97
Ramachandran favored (%)	97.13
Ramachandran allowed (%)	2.80
Ramachandran outliers (%)	0.08
Rotamer outliers (%)	2.20
Clashscore	1.92
Average B-factor (Å^2)	60.63
Macromolecules (Å^2)	60.80
Solvent (Å^2)	52.36
Number of TLS groups	32
PDB ID	**6G1F**

Table S2. X-ray crystallographic data collection and refinement statistics. Statistics for the highest-resolution shell are shown in parentheses.